

Effect of Cr Content on Microstructure and Mechanical Properties of Low Carbon Steel Welds

Hee-jin Lee, Hae-woo Lee*

Department of Materials Science and Engineering, Dong-A University, 840 Hadan-dong, Saha-gu, Busan 604-714, Korea

*E-mail: hwlee@dau.ac.kr

Received: 9 July 2015 / Accepted: 10 August 2015 / Published: 26 August 2015

The effect of Cr content on the formation of acicular ferrite was investigated in low carbon steel welds where submerged arc welding was performed. Three specimens with different Cr content were fabricated and their properties were evaluated. Upon analyzing the microstructure of the welds using optical microscopy, it was observed that a specimen with higher Cr content showed a lower Widmanstätten ferrite content, whereas the proportion of acicular ferrite was increased. Acicular ferrite improves the toughness of welds, and when present in the microstructure, it acts as an obstacle to cleavage fracture. A higher impact absorption energy was measured in a specimen with finer acicular ferrite structures from the impact test. In addition, since Cr is a ferrite-stabilizing element, a higher hardness value was measured for a specimen with higher Cr content. The electrochemical test result showed that as the Cr content increased, the corrosion potential increased and the corrosion current density decreased.

Keywords: metals, welding, mechanical properties, electron backscattering diffraction (EBSD)

1. INTRODUCTION

Recently, the trend in wind power generation is changing from small to large size, from onshore to offshore, and from shallow to deep water. Because the power generation efficiency of offshore wind power is much higher than that of onshore wind power and is superior in production as well, the future wind power market is expected to switch to offshore wind power. In addition, owing to worldwide policies for the growth of new and renewable energy applications, the offshore wind power generation market will grow rapidly, and consequently, the installation of offshore wind turbines is forecasted to increase in future. When installing an offshore wind turbine in shallow seas, the work can be performed by using a barge with drilling equipment since a fixed structure is used. Recently,

various dedicated offshore wind power installation vessels are being proposed because offshore wind power structures with integrated upper and lower parts are being developed. Jack-up leg, usually used in offshore wind power structures, has a diverse range of applications. For legs used in offshore wind power installation vessels and jack-up rigs for drilling, development of steel welding technology for ultra-thick plate is necessary since an increase is expected in the demand for new offshore structures because of increased safety and environmental regulations. Since jack-up leg and rack & chord, which are core components of a wind power installation barge, a high value-added special vessel, are all dependent on foreign countries, their domestic development in South Korea is urgently required. In addition, since an offshore structure stays at one place for a long time once installed, there are limitations on the maintenance and repair when equipment fails. The environments where offshore structures are installed are mostly extreme locations with temperatures as low as -40°C , and deep seas compared to those of ships. Because they are exposed to much wider external environments, excellent performance is required. Therefore, the rack & chord used in offshore structures must be manufactured with high precision. To be used as offshore structures in accordance with such trends, the low temperature toughness evaluation of steel is important. In the case of deep seas, ultra-high pressure resistance must be excellent.[1,2]

In this study, three specimens of welds were fabricated by changing the Cr content in low carbon steel, and their properties were evaluated to determine their suitability for jack-up leg. Cr is an element that increases the strength of welds and their ability to harden, and is known as an element that promotes an increase in the proportion of acicular ferrite. Acicular ferrite has a desirable microstructure, increasing the toughness and strength of welds.[3,4] Therefore, this study was conducted to investigate the effect of Cr addition on the formation of acicular ferrite at welds. Using an optical microscope, changes in the microstructure with Cr content were observed, and through electron back scattering diffraction (EBSD), the crystallographic structure and crystal grain size distribution were determined. Through a tensile test and Charpy-V Notch impact test, the effect of acicular ferrite on the mechanical properties was examined, and through an electrochemical test, the corrosion resistance was evaluated.

2. TEST METHOD

2.1 Welding materials and conditions

The base metal used in this study was SA516-70 steel. With the steel substrates touching each other, submerged arc welding (SAW) was performed using three welding rods with different Cr content. The specimens were collected 20 mm from the weld bead and analyzed. The chemical compositions of the specimens are shown in Table 1. Welding was performed using direct current and reverse polarity, and the preheating temperature of welding was set at 120°C . Specific welding conditions are shown in Table 2.

Table 1. Chemical composition of weld metal (wt%)

	C	Si	Mn	P	S	Cr	Mo	Ni
No. 1	0.10	0.25	1.45	0.007	0.004	0.44	0.41	2.11
No. 2	0.10	0.25	1.45	0.007	0.004	0.23	0.41	2.11
No. 3	0.10	0.25	1.45	0.007	0.004	0.02	0.41	2.11

Table 2. Welding condition

Manufacture	Dia (mm)	Current (A)	Voltage (V)	Welding speed (mm/sec)	Heat input (kJ/mm)
No. 1					
No. 2	4.0	600	30	5	3.6
No. 3					

Preheating Temperature: 120°C
Inter pass Temperature: 150°C
Shielding gas: 80% Ar + 20% CO₂
Polarity: DCEP

2.2 Observation of the macro and microstructure

To observe the macro and microstructures of each weld, machine processing, grinding, and polishing were performed. The macrostructures were observed using a low-magnification microscope after corroding for 10 s with Nital 3%, and the microstructures were observed using an optical microscope after corroding with Nital 7%. The crystallographic structure and crystal grain size distribution were determined using EBSD.

2.3 Mechanical property evaluation

For the hardness measurement of welds, a micro Vickers hardness tester, FV-700 was used. Here, the test load and dwell time were set at 500 gf and 10 s, respectively, and the hardness measurement was performed at the center of the weld at 1 mm intervals. The impact test was conducted at -20°C, -40°C, and -60°C for each specimen by using the Charpy V-notch impact tester, and the tensile test was conducted by collecting the tensile specimens from the deposited metal in parallel with the welding direction according to ASTM A 370-11.

2.4 Electrochemical test

To evaluate the corrosion properties of specimens with different Cr content, a potentiodynamic polarization test was performed using the VersaSTAT 3 (Potentiostat Galvanostat, Princeton Applied Research) equipment. The specimen tested was the working electrode, and platinum foil and silver-silver chloride electrode (Ag, AgCl/KCl) were used as the counter and reference electrodes,

respectively. The electrochemical test was conducted in 0.1 M HCl aqueous solution, between -1 V and 1 V and a scan rate of 1 mV/s.

3. RESULTS AND DISCUSSION

3.1 Macrostructure

Cross-sectional macrostructures of the weldments formed using SAW are shown in Fig. 1. Compared to the heat-affected zone on the base metal side right next to the fusion line, the heat-affected zone formed between the weld layers during multi-pass welding showed noticeable differences in the microstructure as well as impact properties. The grain-coarsening region of the heat-affected zone in the base metal side is the most vulnerable in the weld. On the other hand, at the heat-affected zone produced inevitably between weld layers during multi-pass welding, the impact value and strength are improved by decomposition of the grain boundary ferrite and the Widmanstatten ferrite, which are vulnerable structures, to fine polygonal ferrite and pearlite, which have relatively excellent toughness. [5–7]

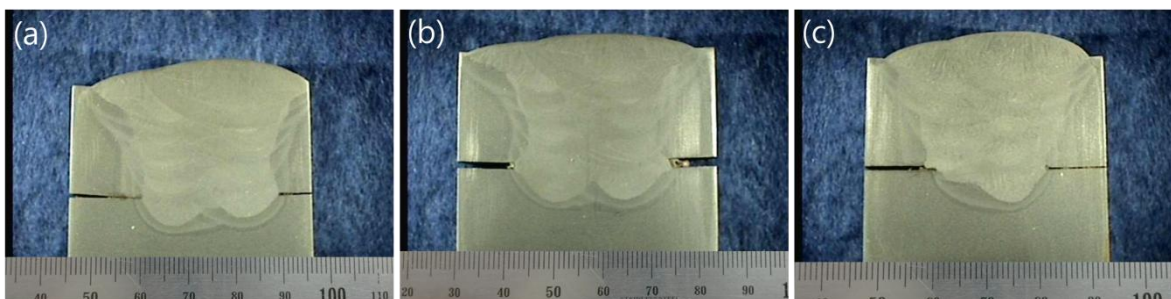


Figure 1. Macrostructures of weldment (a) No. 1, (b) No. 2, (c) No. 3

3.2 Microstructure analysis

3.2.1 Microstructure of weld according to added amount of Cr

Cr is a ferrite-stabilizing element and an element that increases the strength of the weldment and its ability to harden. However, Cr is known to promote the increase the proportion of acicular ferrite, while adversely affecting the toughness. [3] In addition, when the concentration of Mn is low, Cr has a better influence on the weld structure, and because repulsive forces act between the Cr atoms and Mo atoms in the steel when Mo and Cr are added together, acicular ferrite becomes evenly distributed, and a fine structure can be obtained. [3, 8] In Fig. 2, changes in microstructure according to the Cr content can be observed. From (a) to (c), the Widmanstatten ferrite structure is dominant, and the proportion of acicular ferrite decreases. This is because specimen No. 3 contains less Cr than specimen No. 1.

In addition, the grain size of the microstructure, crystal orientation distribution, and phase fraction were measured using EBSD. The crystal orientation distribution is shown in Fig. 3, which shows the IPF (Inverse Pole Figure) maps of EBSD, and the crystal orientation distribution is viewed as different colors. Growth is observed in the [100], [110], and [331] directions of acicular ferrite. [9] It is observed that the grain size increases from (a) to (c) in Fig. 3. In the next section, the effect of microstructure on the mechanical properties, examined through the grain size distribution and phase map using EBSD, is discussed.

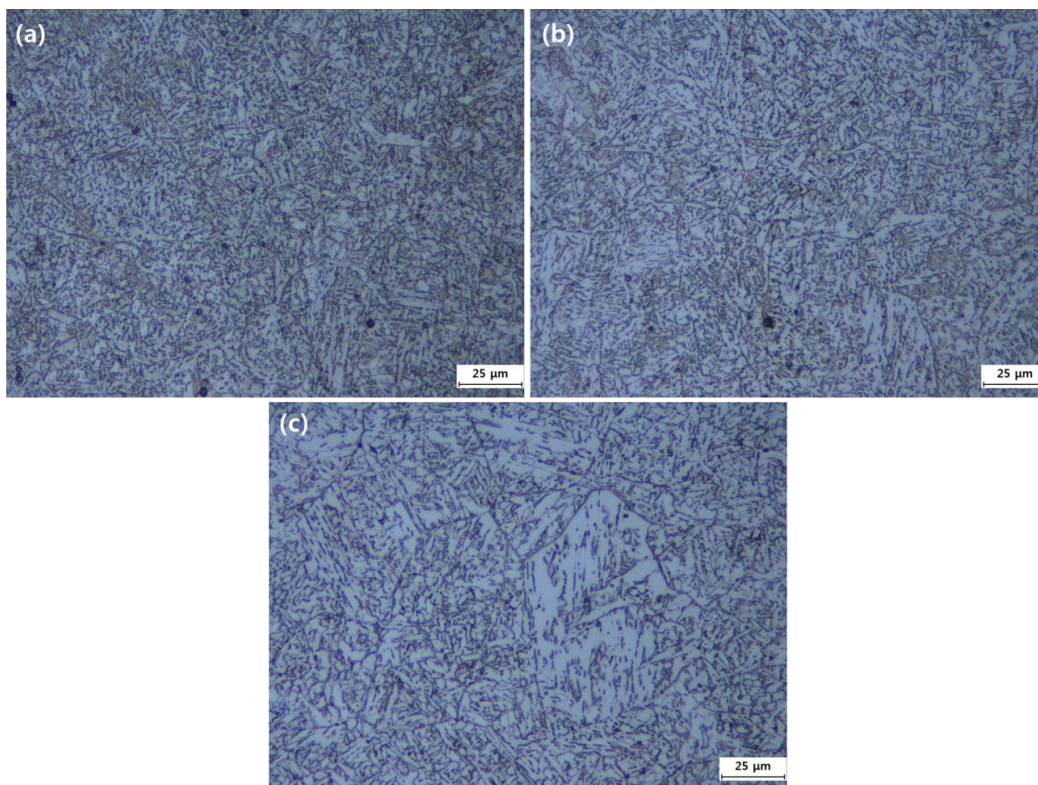
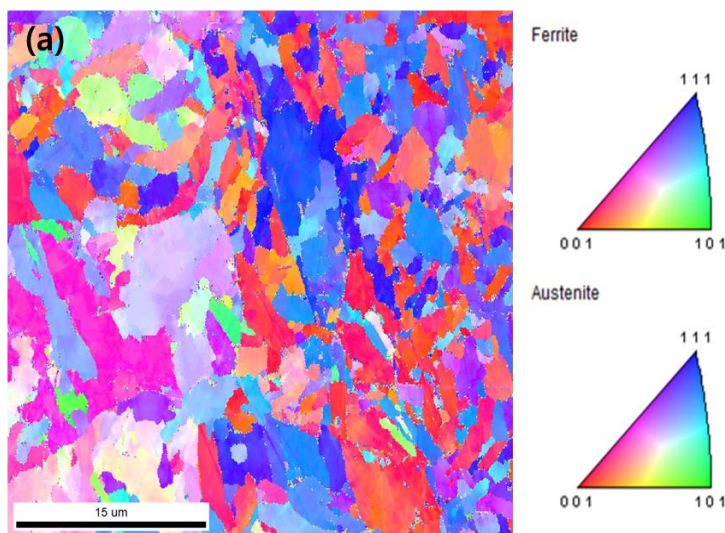


Figure 2. Microstructure of welds (a) No. 1, (b) No. 2, (c) No. 3



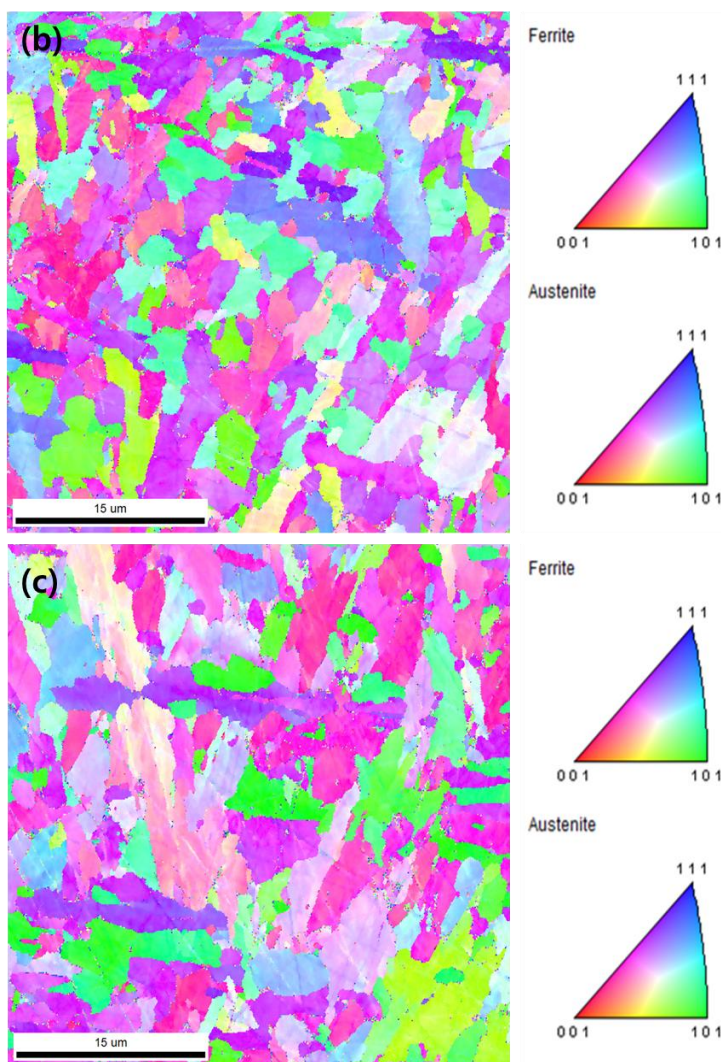


Figure 3. EBSD inverse pole figure map of weld metal (a) No. 1, (b) No. 2, (c) No. 3

3.2.2 Effect of acicular ferrite

Acicular ferrite is known to increase the toughness and strength of the weldment. [10] Acicular ferrite, which is a thin and fine ferrite, exists in an irregular arrangement between the crossed austenite. The disordered grain boundaries of non-parallel acicular ferrite hinder the spread of cracks and affect the toughness improvement of the weldment. [11–14] Acicular ferrite is formed usually in the weld inclusion at 500–650°C. [14, 15] For the formation of acicular ferrite, an inclusion activating intragranular nucleation is required. The oxygen and nitrogen inclusions have an important influence on the nucleation of acicular ferrite. In a spherical inclusion, nucleation occurs to form the acicular ferrite. Acicular ferrite was originally assumed to be a type of Widmanstätten ferrite. [16, 17] However, currently, it is understood to be a type of bainite. Nucleation of acicular ferrite occurred in the inclusions, and the growth is limited because of collisions with other acicular ferrites formed in the early austenite grain boundary. Bainite is different from acicular ferrite in that it is formed in locations other than inclusions inside the grains. [14, 15] Acicular ferrite is related to the presence of an adequate amount of inclusions in the austenite grains, and if the inclusion is not present, it is known

that the acicular ferrite is not formed well. [8] Therefore, if the inclusion does not exist, more bainite will be formed compared to acicular ferrite. If bainite is also present inside the microstructure, it will hinder crack propagation and will aid the toughness of the weldment, but it will not be more effective than acicular ferrite.

Furthermore, as shown in Fig. 4, the acicular ferrite exists mutually interlocked with the Widmanstätten ferrite. The irregular arrangement of the ferrite plate increases the toughness of the weldment, and it is reported that because of the crystallization and disorder of acicular ferrite a better toughness is observed compared to bainite. [18, 19] The inclusions for nucleation of acicular ferrite decrease elements such as C, Mn, and Si of austenite. Such a decrease in the elements leads to an increase in the driving force for nucleation on the inclusion surfaces.[20]

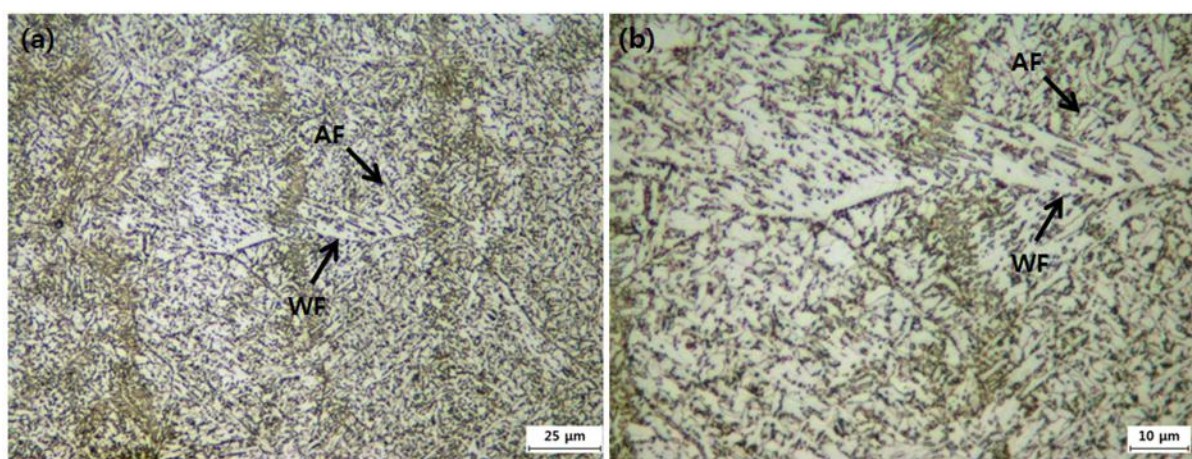


Figure 4. Acicular ferrite and Widmanstätten ferrite microstructure in weld metal (a) 500x, (b) 1000x

3.3 Impact properties

Fig. 5 shows the impact test results at test temperatures of -20°C , -40°C , and -60°C . As shown in the graph, a specimen with more Cr had higher absorbed energy. The value of the absorbed energy in the impact test is the energy required to fracture the specimen. Cr is a ferrite stabilizing element and an element promoting the increase in the acicular ferrite fraction inside the weldment. Acicular ferrite is a desirable structure from a toughness aspect for resisting impact because the grains are fine and dense. Therefore, a specimen with higher Cr content has a higher impact energy because the acicular ferrite content is increased.

As shown in the measurement results of Fig. 6, when the Cr content was high, the distribution of fine grains was high. The high density of fine grains forcefully changes the cleavage fracture to fine planar propagation and acts as an obstacle for the propagation of cleavage fracture. Therefore, when a specimen had a lower Cr content, a low impact absorption energy was measured in the impact test. Furthermore, at -20°C , the highest absorbed energy was measured, and when the test temperature decreased, the impact absorption energy of the specimen decreased. This can be explained by Peierls stress that analyzes the movement of electric potential. [21] Peierls stress is the stress required in

moving a dislocation in crystal. This stress is related to the yield strength and temperature. As the temperature drops, the movement of potential is slowed down and the force required in moving the potential becomes larger, increasing the Peierls stress and the yield strength of the material. In other words, the yield strength and the toughness of a material are inversely related. Therefore, as the temperature drops, a lower absorbed energy is observed.

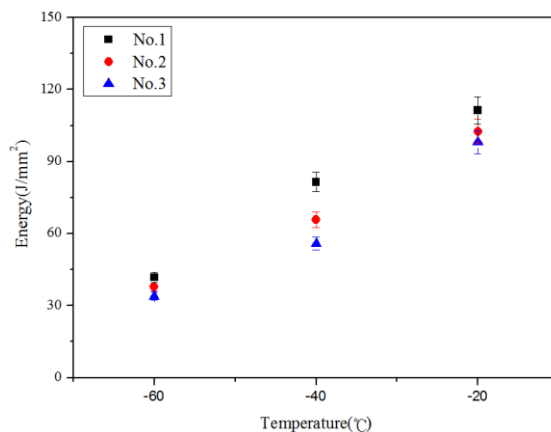


Figure 5. Results of Charpy V-notch impact tests for weldments

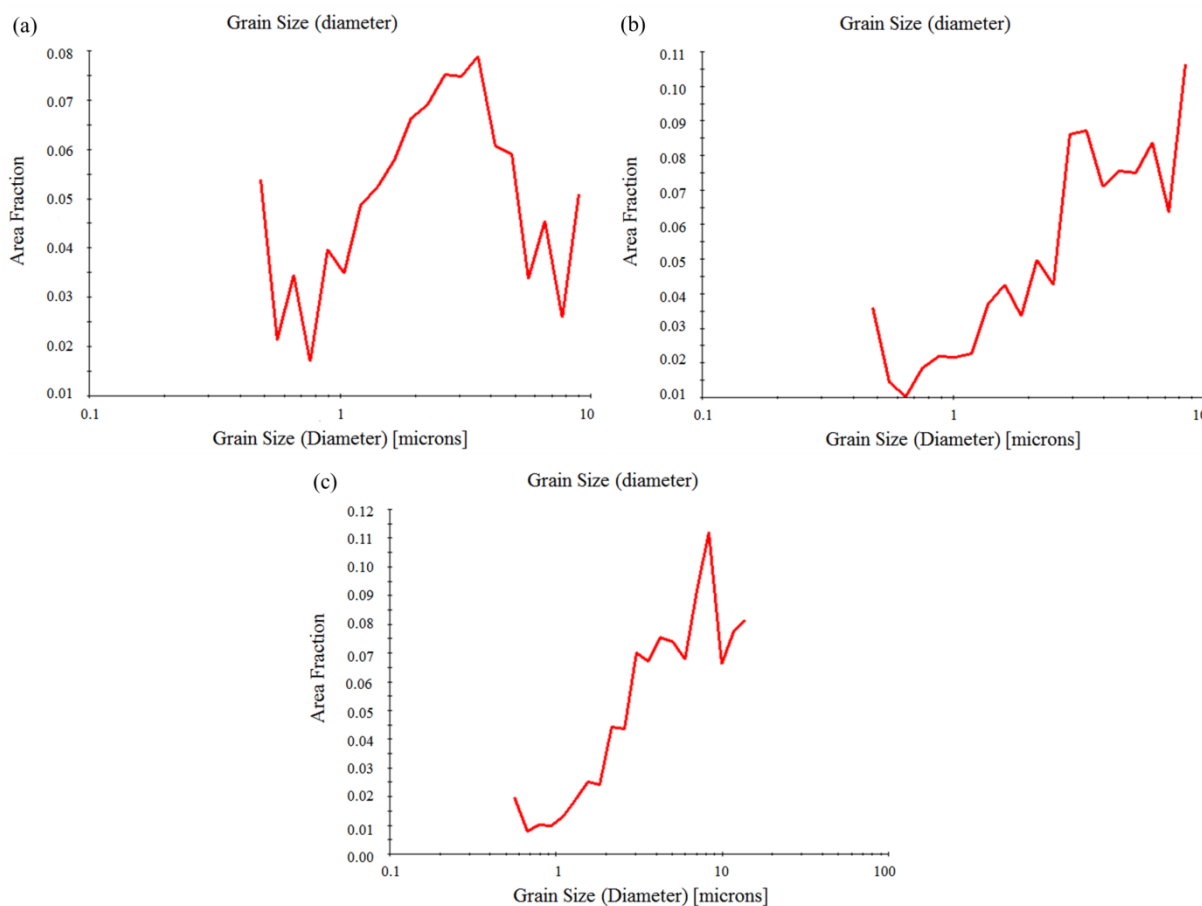


Figure 6. EBSD grain size distribution of weldments (a) No. 1, (b) No. 2, (c) No. 3

3.4 Tensile strength and hardness

In Fig. 7, the tensile test results of the weldment, i.e., yield strength, tensile strength, and elongation are shown. It can be seen that the yield strength of No. 1, No. 2, and No. 3 specimens increase gradually. This is because of the differences in the Cr content. When a specimen has more Cr, the fraction of acicular ferrite increases, and disordered arrangements of such acicular ferrite hinder the propagation of cracks and affect the toughness improvement of the weldment. However, the toughness and the yield strength are inversely related. Therefore, because a specimen with higher Cr content has a larger amount of acicular ferrite with excellent toughness, it was observed that the yield strength value is low in the tensile test result.

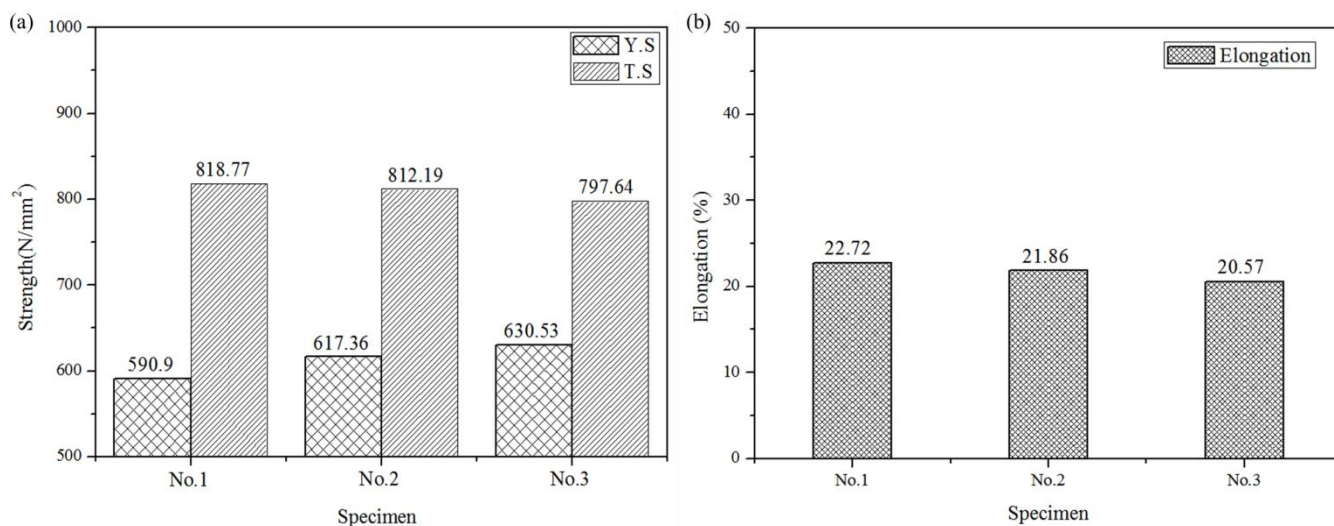


Figure 7. Tensile strength test results (a) Tensile strength and Yield strength, (b) Elongation

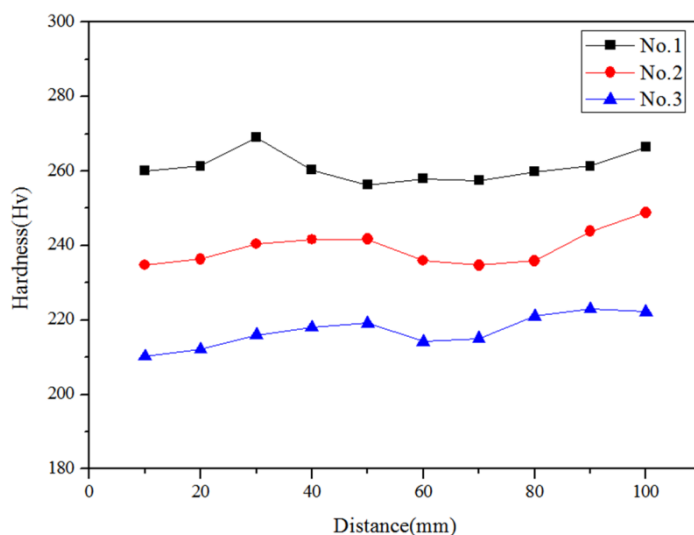


Figure 8. Hardness of weld metals

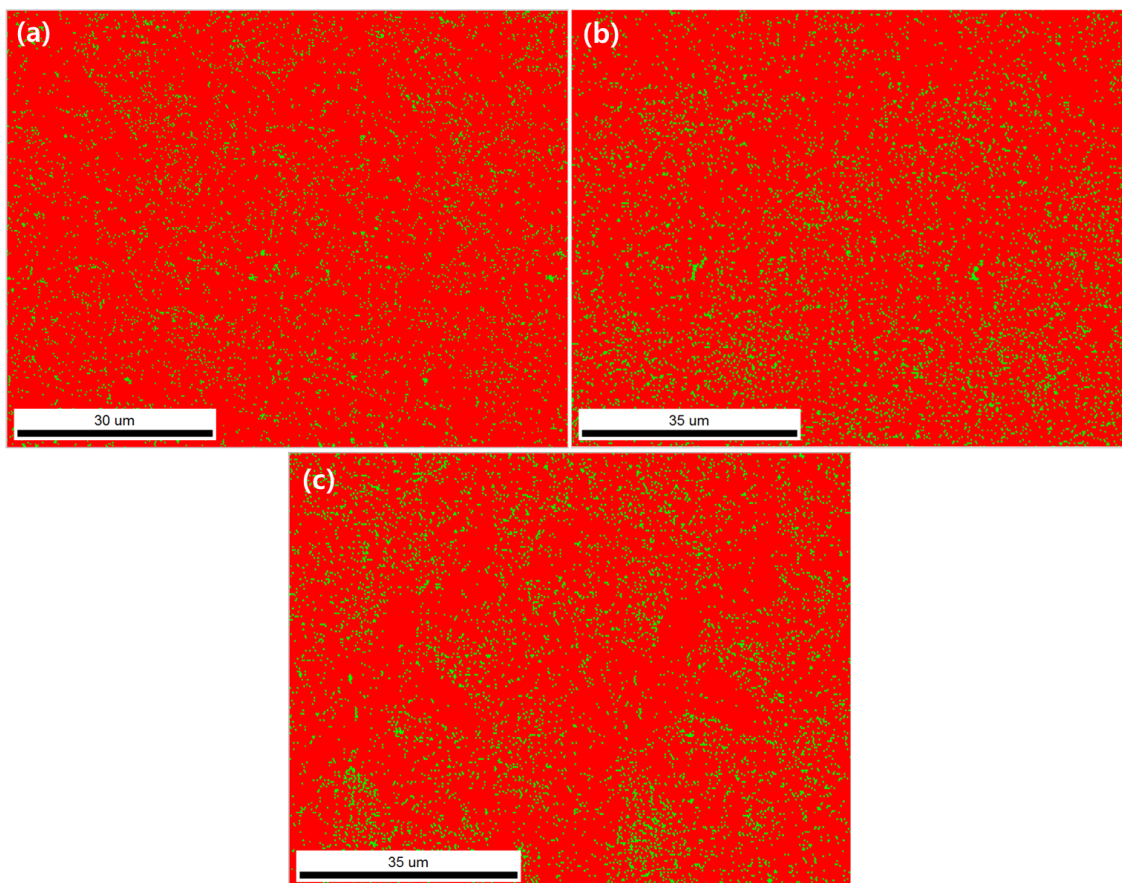


Figure 9. EBSD phase map of weld metals (a) No. 1, (b) No. 2, (c) No. 3

Fig. 8 shows the measured values of hardness for each weld metal. Specimen No. 1 has the relatively highest hardness value. It seems that higher the Cr content, the higher is the hardness value. This result can be explained by analyzing the results of Fig. 8 and Table 3. Fig. 9 is a result of the analysis of the phase of weld metals through phase maps. The red color shows the ferrite and the green color shows the austenite, and the fraction of each phase is shown in Table 3. When a specimen has a higher Cr content, it can be confirmed that the fraction of ferrite is higher, and in general, ferrite is known to have a higher strength than the austenite structure. As a result, the hardness of specimen No. 1, with a high ferrite content because of Cr, was higher.

Table 3. Phase fraction of the weld metals (%)

Specimens	Fraction of Ferrite	Fraction of Austenite
No. 1	94.4	5.6
No. 2	91.6	8.4
No. 3	91.2	8.8

3.5 Electrochemical Test

Fig. 10 exhibits a potentiodynamic polarization curve of each specimen in 0.1 M HCl. A passive state is not formed in every specimen, and an active corrosion behavior is observed whereby the current density increases according to the increase in potential. Since Cl⁻ present in the aqueous solution changes the water solubility of a passive state film, no passive state is observed. In the corrosion test performed, a typical polarization behavior of uniform corrosion is observed whereby the dissolved Fe cations are converted into an oxide on the surface of the electrode and corrosion occurs evenly on the entire surface of the specimen. [22–24] Corrosion potential (E_{corr}), corrosion current density (I_{corr}), β_c , and β_a which are corrosion parameters can be obtained by expanding the Tafel region on the polarization curve, and the results are shown in Table 4. It has been reported that in general, Cr forms Cr oxide, which is a surface oxide, and enhances the corrosion resistance of the alloy in salt solution. [25-27] The Cr oxides resulting from the addition of Cr reduced oxidation and reduction reactions. [28] As shown in the corrosion test results of Table 4, as the Cr content increased, the corrosion potential increased and the corrosion current density decreased. Similar to previous reports, the specimens of the corrosion test performed in this study did not have a large enough difference in Cr content to show a clear degree of corrosion.

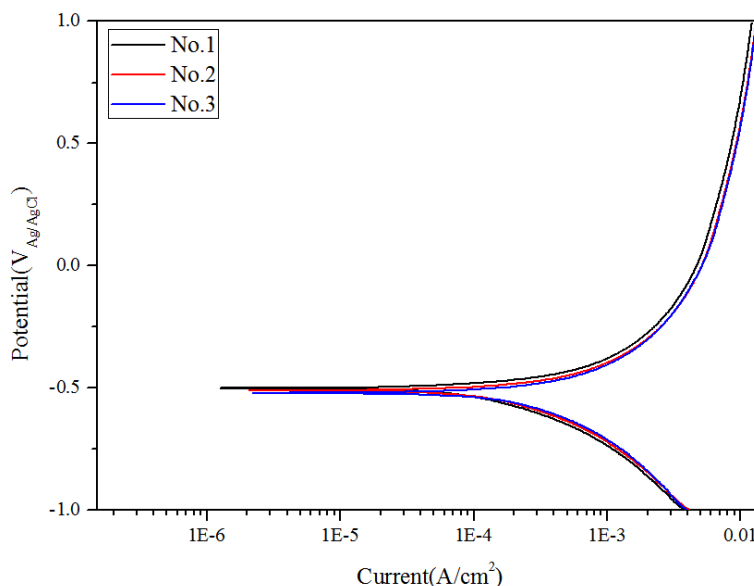


Figure 10. Corrosion test results of weld metal in 0.1 M HCl

Table 4. Corrosion potential and current of weld metal

Specimens	E_{corr} (mV)	I_{corr} ($\mu\text{A}/\text{cm}^2$)	β_c (mV/dec)	β_a (mV/dec)
No. 1	-500.920	241.625	418.274	224.811
No. 2	-510.965	429.239	596.667	286.188
No. 3	-520.827	679.606	811.338	383.412

4. CONCLUSION

The microstructure and mechanical properties of low carbon steel welds with Cr addition are as follows.

1. Cr is an element that increases the strength of welds and their ability to harden, and promotes an increase in the proportion of acicular ferrite. From the microstructural analysis, more acicular ferrite was observed at the weldment in a specimen with higher Cr content.
2. Since acicular ferrite improves the toughness and strength of a weldment, as it becomes finer, it acts as an obstacle for cleavage fracture. In the grain size distribution using EBSD, a specimen with higher Cr content showed a higher micrograin distribution. Therefore, when the Cr content increased, a higher absorbed energy was measured in the impact test results.
3. Since the toughness and yield strength are inversely proportional, the value of yield strength obtained from the tensile test is low for a specimen in which a high fraction of acicular ferrite was formed because a large amount of Cr was added. In addition, because Cr is a ferrite-stabilizing element, the measured hardness value of a specimen with higher ferrite content was higher.
4. The result of the electrochemical test shows that as the Cr content increases, the corrosion potential increases and the corrosion current density decreases.

ACKNOWLEDGEMENT

This investigation was supported by the Dong-A University Research Fund.

References

1. European Committee for Standardisation, Eurocode 3: Design of steel structures – Part 1-10: Material toughness and through-thickness properties (2005)
2. I. P. Kim, Y. Heo, Y. S. Park and T. Y. Yoon, *J. KSCE*, 56(10) (2008), 59
3. J. C. F. Jorge, L. F. G. Souza, J. M. A. Rebello and G. M. Evans, *Mater. Charact.*, 47(3) (1992), 195
4. R. A. Ricks, P. R. Howell and G. S. Barritte, *J. Mater. Sci.*, 17(3) (1982), 732
5. A. Joarder, S. C. Saha and A. K. Ghose, *Welding Research Supplement*, 70 (1991), 141
6. C. L. Jenney and A. O'Brien, *Welding Handbook*, Vol. 1(8th), pp. 368, American Welding Society (1987)
7. J. H. Jeon, J. Y. Hong and H. W. Lee, *Korean J. Met. Mater.*, 51(1) (2013), 033
8. M. Honjo and Y. Saito, *ISIJ*, 40 (2000), 914
9. R. A. Farrar and P. L. Harrison, *J. Mater. Sci.*, 22 (1987), 3812
10. S. Babu, Ph.D. Thesis, pp. 1–15, University of Cambridge, England (1991)
11. S. W. Kang, M. H. Kim, W. T. Shin and H. W. Lee, *J. SNAK*, 41 (2004), 41
12. K. H. Kim, H. J. Kim and M. Y. Huh, *JWJ*, 27 (2009), 14
13. G. L. F. Powell and G. Herfurth, *Metall. Mater. Trans. A*, 29A(11) (1998), 2775
14. G. Thewlis, *Mater. Sci. Tech.*, 2(10) (1994), 110
15. J. H. Tweed and F. F. Knott, *Acta Metall.*, 35(7) (1987), 1401
16. S. W. Thompson, D. J. Colvin and G. Kraus, *Metall. Mater. Trans.*, 27A(6) (1996), 1557
17. H. K. D. H. Bhadeshia, *Bainite in steels*. 2nd ed. Carlton House Terrace, London: IOM Communications Limited (2001)
18. M. Diaz-Fuentes, A. Iza-Mendia and I. Gutierrez, *Metall. Mater. Trans. A*, 34A (2003), 2505
19. S. S. Babu, *Curr. Opin. Solid State Mater. Sci.*, 8 (2004), 267
20. J. M. Gregg and H. K. D. H. Bhadeshia, *Acta Metall. Mater.*, 42 (1994), 3321

21. R. Peierls, *Proc. Phys. Soc.*, 52 (1940), 34
22. M. J. Jang, Y. W. Jang, Y. Y. Ha, J. J. Kim and J. K. Kim, *Korean J. Electrochem. Soc.*, 13 (2010), 96
23. D. A. Jones, *Principles and Prevention of Corrosion*, pp.109–132, Prentice Hall, New Jersey (2007)
24. E. M. Sherif, R. M. Erasmus and J. D. Comins, *Electrochim. Acta*, 55 (2010), 3657
25. S. A. Park, W. S. Ji and J. G. Kim, *Int. J. Electrochem. Sci.*, 8 (2013), 7498
26. J. W. Schultze and M. M. Lohrengel, *Electrochim. Acta*, 45 (2000), 2499
27. P. Schmuki, *J. Solid State Electrochem.*, 6 (2002), 145
28. S. W. Kim and H. W. Lee, *Int. J. Electrochem. Sci.*, 9 (2014), 4709

© 2015 The Authors. Published by ESG (www.electrochemsci.org). This article is an open access article distributed under the terms and conditions of the Creative Commons Attribution license (<http://creativecommons.org/licenses/by/4.0/>).